UNIVERSITY OF TARTU
Institute of Computer Science
Computer Science Curriculum

Michelle Lukken

Feasibility Study of Performing the DC Magnetic Field Emission Test for QPIC with Helmholtz Coils in Tartu Observatory

Bachelor's Thesis (9 ECTS)

Supervisor:
Sten Salumets, M.Sc.

Tartu 2025

Feasibility Study of Performing the DC Magnetic Field Emission Test for OPIC with Helmholtz Coils in Tartu Observatory

Abstract:

The OPIC space instrument, which is developed by Tartu Observatory, needs to be thoroughly tested before launch. One of the required tests is the DC Magnetic field emission test. Since doing it elsewhere is more time consuming and expensive, it is preferred to do this in-house. Although Tartu Observatory has Helmholtz coils, they have not been thoroughly tested and have minimal documentation. The thesis aims to study the feasibility of performing this test with existing hardware. During the thesis, the author developed control logic for Helmholtz coils and made additional hardware for magnetometer placement. Furthermore, the author tested the stability and uniformity of the created magnetic field and analyzed the hardware's suitability for the test.

Keywords: OPIC, Helmholtz, Electromagnetic compatibility, ECSS standard

CERCS: P180 Metrology, physical instrumentation, P200 Electromagnetism, optics, acoustics, T320 Space technology[1]

Teostatavusuuring Helmholtzi poolidega OPICu alalisvoolu magnetvälja emissioonitesti teostamiseks Tartu Observatooriumis

Lühikokkuvõte:

Tartu Observatooriumi poolt välja töötatud kosmoseaparatuur OPIC vajab enne lennustarti põhjalikku testimist. Üks vajalikest testidest on alalisvoolu magnetvälja emissiooni test. Kuna mujal testide tegemine on aeganõudvam ja kulukam, on eelistatud seda teha majasiseselt. Kuigi Tartu Observatooriumis on Helmholtzi poolid olemas, pole neid põhjalikult testitud ja nende kohta on minimaalselt dokumentatsiooni. Lõputöö eesmärk on uurida testi teostatavust olemasoleva riistvaraga. Lõputöö käigus töötas autor välja Helmholtzi poolide juhtimisloogika ja valmistas täiendava riistvara magnetomeetri paigutamiseks. Lisaks testis autor loodud magnetvälja stabiilsust ja ühtlust ning analüüsis riistvara sobivust testiks.

Võtmesõnad: OPIC, Helmholtz, Elektromagneetiline ühilduvus, ECSS standard

CERCS: P180 Metroloogia, instrumentatsioon, P200 Elektromagnetism, optika, akustika, T320 Kosmosetehnoloogia[1]

Contents

Acronyms

AC Alternating Current. 31

CAD Computer-Aided Design. 17

CSV Comma-Separated Values. 26

DC Direct Current. 3, 5, 11, 13, 31, 32

ECSS European Cooperation for Space Standardization. 5, 11

EMC Electromagnetic Compatibility. 5, 11

ESA European Space Agency. 6, 11

FPGA Field Programmable Gate Array. 7

JAXA Japan Aerospace Exploration Agency. 6

OPIC Optical Periscopic Imager for Comets. 5, 7, 11, 15, 32

PLA Polylactic Acid. 18

VISA Virtual Instrument Software Architecture. 20

1. Introduction

Over the years, precise standards—such as those defined by the European Cooperation for Space Standardization (ECSS)—have been established to ensure that spacecraft and space instrumentation are thoroughly tested before launch[2]. These standards have become essential, as inadequate testing has historically contributed to the failure of numerous space missions[3], [4], [5].

Tartu Observatory is currently developing Optical Periscopic Imager for Comets (OPIC), an instrument for the European Space Agency's (ESA) deep-space Comet Interceptor mission. Similar to any other space mission, OPIC must undergo extensive testing, including mechanical, thermal, optical, functional, and Electromagnetic Compatibility (EMC) assessments. While most of these tests can be conducted using the Observatory's dedicated laboratory facilities, the setup for performing DC magnetic field emissions testing remains undeveloped.

This particular test requires the compensation of Earth's magnetic field and the generation of controlled magnetic environments. One solution is the use of Helmholtz coils — devices capable of producing highly uniform magnetic fields. Three-axis Helmholtz coils, developed by students, have been available at Tartu Observatory for over a decade. Although they have not been actively used or thoroughly tested, they may serve as a foundation for this testing setup.

The goal of this thesis is to explore the feasibility of conducting the DC magnetic field emissions test for OPIC in-house in Tartu Observatory, using the existing Helmholtz coil hardware. To achieve this, the requirements and procedures of the test are studied. The thesis addresses both the software and the hardware necessary to carry out the test successfully.

The preparation of this thesis involved the use of ChatGPT to edit and clarify the expression of ideas. For this purpose, ChatGPT was provided with one or several sentences and prompted to rewrite them for improved clarity or a more academic writing style.

2. Literature review

2.1 Comet Interceptor mission

Until now, only short-period comets—originating from the relatively nearby Kuiper Belt—have been studied by fly-by missions. Notable examples include the Giotto mission in 1986[6], which observed Comet 1P/Halley, and the Rosetta mission from 2014 to 2016[7], which orbited and landed on Comet 67P/Churyumov-Gerasimenko. In contrast, long-period comets—such as those believed to originate from the distant Oort Cloud at the edge of the Solar System—are typically discovered only a few years before reaching perihelion, their closest approach to the Sun. This short lead time makes it extremely challenging to design, build, and launch a spacecraft in time for a meaningful encounter. Comets from the Kuiper Belt have spent considerable time in the inner Solar System and have therefore undergone substantial alteration since their formation. On the other hand, Oort Cloud comets have orbital periods of tens of thousands of years and may be visiting the inner Solar System for the first time. As a result, they are thought to retain more pristine information about the early Solar System, making them particularly valuable for scientific study.[8]

The Comet Interceptor does not focus on a specific comet. It is designed to perform a fly-by of an undiscovered Oort cloud comet or even an interstellar object that is found after its launch. The idea is to put the comet interceptor in an orbit close to the Sun-Earth L2 Lagrange point, which is an equilibrium point between Earth and Sun, that is located approximately 1.5 million kilometers from Earth in the opposite direction as the Sun. In this orbit, the spacecraft can wait a few years for the discovery of a suitable comet that is reachable. After finding a suitable comet, the Comet Interceptor can maneuver to the computed interception point and release two smaller probes (spacecraft B1 and B2) from the mothership (spacecraft A). The spacecrafts are planned to be at different distances from the comet to keep the mothership safe, but also perform riskier measurements closer to the comet. It is planned that the mothership will be 1000 km from the comet, while probes B1 and B2 will study the comet closer at 850 km and 400 km, respectively. By combining data from three spacecrafts it is possible to study the comet from different angles during the fly-by. This mission hopes to gather information about the target comet's surface composition, shape, morphology and structure.[9]

The Comet Interceptor mission is developed by the European Space Agency (ESA) in cooperation with the Japan Aerospace Exploration Agency (JAXA). The mission was proposed to ESA in 2018 and is planned to launch in 2028 together with the Ariel mission[10].

2.2 OPIC project description

OPIC is an instrument aboard the B2 probe of the Comet Interceptor mission. It is developed by Tartu Observatory at the University of Tartu, in collaboration with Crystalspace, an Estonian space technology company serving as the industrial contractor. OPIC represents Estonia's first deep-space scientific instrument.

OPIC is an automated camera system for taking images of the target comet and its near environment. Its aim is to map the comet's nucleus and its surrounding coma and dust environment. For that, the instrument will be gathering, processing, prioritizing and autonomously transmitting the comet images data to the main spaceship. [11]

OPIC is only 5.6 x 16.1 x 7.6 cm in size and consists of an integrated imaging module, a refractive lens assembly, an optical bandpass filter, a periscope that houses a mirror and an integrated baffle. The mirror allows to angle the field of view to enable imaging towards the direction of flight. The instrument is shaped so to hide sensitive parts such as electronics and optics deeper into the spacecraft. The camera has an CMV4000[12] 2048 x 2048 pixel monochrome image sensor and a 3 million gate ProASIC3 Field Programmable Gate Array (FPGA) for image processing and transmission and communications. The engineering model of OPIC can be seen in Figure **1**.

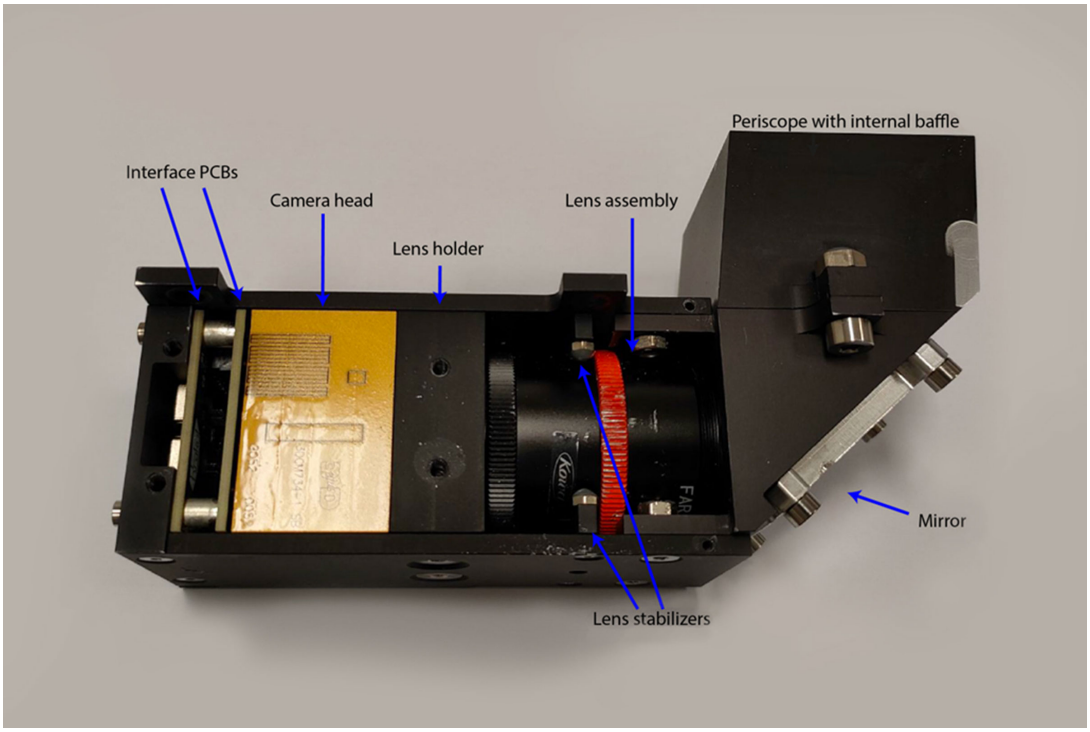

Figure 1. OPIC engineering model [9]

2.3 Magnetic field

Measuring magnetic field emissions begins with understanding the concept of a magnetic field. It is a physical field, which is produced by an electrical current. An electrical current produces a magnetic field in a plane perpendicular to itself. For example, current I flowing in a direction $\vec{z}$ creates a magnetic field in a x-y plane[13]. A piece of wire with a constant current produces a magnetic field described by Biot-Savart law [14]:

$$\vec{B}(\vec{r}) = \frac{\mu_0 I}{4\pi} \int \frac{d\vec{l}' \times (\vec{r} - \vec{r}')}{|\vec{r} - \vec{r}'|^3}$$

- $\vec{B}(\vec{r})$ is the magnetic field at point $\vec{r}$
- I is the current through the wire
- μ_0 is the permeability of free space ($\mu_0 = 4\pi \times 10^{-7}$ T $\cdot$ m/A)
- $d\vec{l}'$ is a differential vector element of the wire at position $\vec{r}'$
- $\vec{r} - \vec{r}'$ is the vector from the wire element to the field point
- The integral is over the entire wire

The SI unit of magnetic field is the tesla, symbolized as T but it is also commonly measured in gauss, where 1 Tesla is equal to 10^4 gauss.

2.3.1 Earth's magnetic field

When measuring an object's magnetic field on Earth, it needs to be taken into account that the measurement also includes the Earth's magnetic field. Earth has a magnetic field, that is created from multiple contributing factors:[15]

- The main field, that is created by geodynamo mechanism in the Earth's fluid core
- The crustal field, that is generated by magnetized rocks in Earth's crust.
- The external field, that is produced by electric currents flowing in the ionosphere and magnetosphere and is influenced by solar electromagnetic radiation and solar wind.
- The magnetic field created by electromagnetic induction, that is generated by electric currents induced in the crust and upper mantle by external magnetic field time variations

These together create a magnetic field with a strength ranging between 22 to 67 microTeslas[16]. This magnetic field influences other magnetic fields on Earth.

2.3.2 Magnetic fields and ferromagnetic properties

Magnetic fields can be used to influence ferromagnetic materials. Controlled magnetic fields can demagnetize or polarize objects. Ferromagnetic materials are magnetised in the presence of a magnetic field. If they have high coercivity they retain this magnetisation. This affects the measurement.[17]

Magnetisation can be removed using a process called deperming. Deperming is the process of removing or decreasing a permanent magnetic field. This can be done by creating an oscillating magnetic field with decreasing amplitude in a magnetic field-compensated environment. The reverse process of this is perming, that creates a permanent magnetic field. This can be done by creating a stable magnetic field with a desired field strength. After perming ferromagnetic materials have a residual magnetic field around them, called stray field. Stray field can be measured to evaluate their impact on nearby systems. These processes can be performed on a ferromagnetic object by controlling the magnetic field around it.[18]

2.4 Helmholtz coils

Helmholtz coils are a pair of circular coils that have equal diameter and number of turns. The coils are located coaxial to each other at a distance h, that is equal to the common radius r of the coils. This arrangement can be seen in Figure **2**. The main usage of Helmholtz coils is to create custom magnetic fields: compensate the Earth's magnetic field, create a stable or switching field in between the coils. Helmholtz coils can be used to produce a nearly uniform magnetic field in a region surrounding the center point of the axis between two coils as seen in Figure **3**.[19]

Magnetic field produced by a single coil at a distance z from the coil along the axis can be described by the special case of Biot–Savart law mentioned above:

$$B(z) = \frac{\mu_0 I r^2}{2(r^2 + z^2)^{3/2}}$$

- μ_0 is the permeability constant that is equal to $4\pi \times 10^{-7} T \cdot m/A = 1.257 \cdot 10^{-6} T \cdot m/A$
- I is the coil current in ampers
- r is the coil radius in meters
- z is the coils distance on axis to the point in meters

When looking at Helmholtz coils the total magnetic field is the sum of the magnetic fields created by two coils: $B_{total} = B_{coil1} + B_{coil2}$.

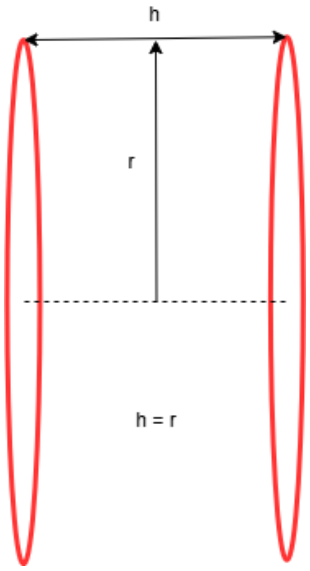

Figure 2. Helmholtz coil pair

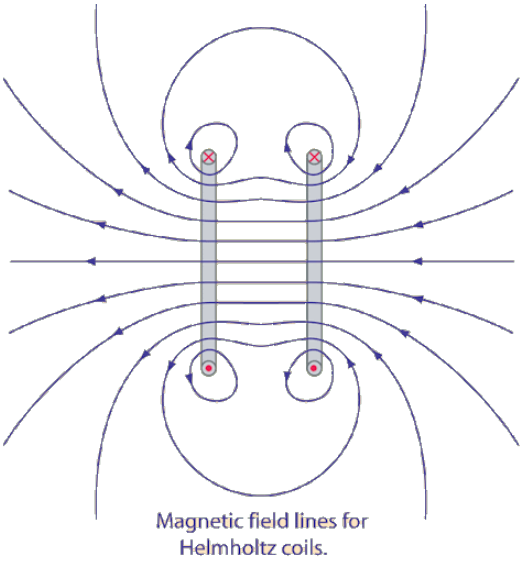

Figure 3. Magnetic filed lines inside Helmholtz coil pair[20]

Magnetic field created by Helmholtz coils with N turns can be described by following formula:

$$B(z) = \frac{\mu_0 N I r^2}{2} \cdot \left[\frac{1}{(r^2 + (z + \frac{r}{2})^2)^{3/2}} + \frac{1}{(r^2 + (z - \frac{r}{2})^2)^{3/2}} \right]$$

In the center of the Helmholtz coils, $z = 0$: $B(0) = (\frac{4}{5})^{3/2} \cdot \frac{\mu_0 N I}{r}$.

One pair of Helmholtz coils creates uniform field in only one axis. To have uniform field in three directions, three pairs of coils must be used, as seen in Figure **4**. For testing instruments it is needed to control magnetic fields in all three axes.

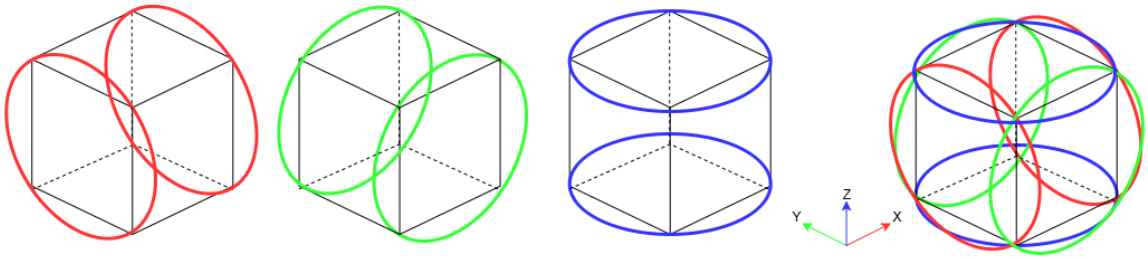

Figure 4. Helmholtz coil pairs in X, Y, Z direction and combined

2.5 Electromagnetic compatibility standard

Space systems need to be tested before launch to confirm that they conform with the overall mission requirements and objectives, ensuring functionality and reliability. For testing space systems, standardized procedures have been developed. As OPIC is an instrument for an ESA mission, the ECSS is followed[2].

The OPIC qualification tests are performed in several categories, each following different standardization. The team at Tartu Observatory has developed setups to perform mechanical, thermal, optical, functional, and EMC tests as to qualify the developed instrument. This thesis focuses on studying the DC magnetic field emission test, which falls under the EMC test category. The test needs to follow the ECSS Electromagnetic compatibility standard (ECSS-E-ST-20-07C) of which the latest revision 2 was published in January 2022. [21]

2.5.1 Description of the DC Magnetic Emission Test

The purpose of the DC Magnetic field emission test is to measure the magnetic moment M of the instrument. The magnetic moment mission requirement for OPIC is less than $0.001 Am^2$. This is a strict requirement due to the presence of an FGM instrument, a dual-sensor fluxgate magnetometer, positioned next to OPIC on Probe B2[9]. Higher magnetic emissions from OPIC could interfere with the measurements of FGM.

For the test procedure magnetic sensors are used to measure the magnetic field around the instrument. According to the testing procedure it is required to use single-axes magnetometers as the magnetic field sensors. To get more uniform measurements, two magnetometers should be used. These magnetometers m_1 and m_2 should be placed at different reference distances r_1 and r_2 from the geometric centre of the instrument, that marked with a square in Figure **5**. In the figure magnetometers X-axis coils are red and Y-axis coils are green.

Tartu Observatory already had two high quality AlphaLab Inc.'s Milligauss Meter MR3 magnetometers. These magnetometes can measure three vector components (X, Y and Z) as well as magnitude of the magnetic field and can stream data live via a USB connector. They can measure the magnetic field between 1999.99 and -1999.99 milligauss with a resolution of 0.01 milligauss (1 nanoTesla). Maximum error of sensitivity is +/- 0.5 % of the reading, and the maximum error of the offset is +/- 0.50 milligauss[22]. The confirmation of the suitability of these magnetometers was also received from the ESA senior EMC advisor Johannes Wolf.

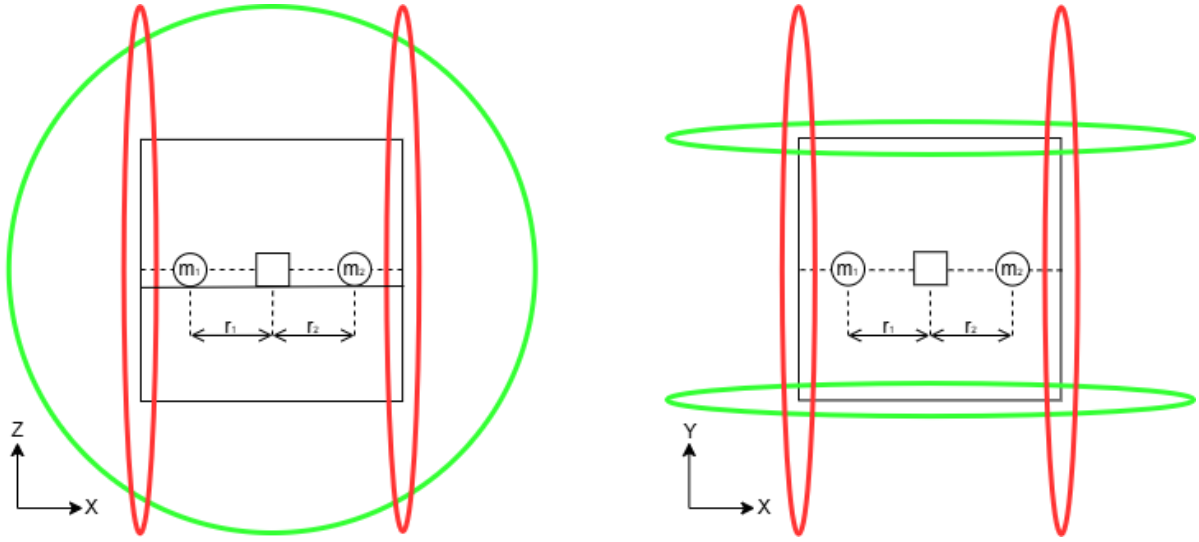

Figure 5. Magnetometer placement inside Helmholtz coil viewed from Y- and Z-axis

The testing should take place in an Earth field compensated area, meaning that a magnetic field needs to be generated, which can modify the magnitude of the Earth's magnetic field to be zero. Then, with the Earth field compensated area, it would be possible to measure the unit under test's own magnetic emissions without an external field. One option to compensate Earth's magnetic field is to use Helmholtz coils, described in section 2.4.

2.5.2 Test sequence

According to ECSS-E-ST-20-07C[21], the test needs to be performed in five separate steps. For most of the measurements the instrument should not be operating. Further information about the magnetic fields created in different steps can be found in section 2.3.2. The steps are following:

1. Measuring the instrument by using two magnetometers within the Earth-compensated area.
2. Eliminating the magnetic field through the deperming process. This involves generating an oscillating magnetic field with a frequency between 2.5 and 5 Hz and a peak amplitude of 4000 to 5000 microTeslas. Changing the magnetic field in such a manner should remove the magnetisation of the instrument. After deperming, the instrument should not have any remnant magnetic field.
3. Creating a permanent field of 300 uT for all axes and measuring the field, a field that is 5 to 10 times stronger than the Earth's magnetic field.

4. Measuring the operating instrument with a stray field from the previous part. This should help identify the magnetic field created around the instrument.

5. Performing a second deperming using the same parameters as before to ensure the instrument returns to a demagnetized state.

These five steps are repeated on all six axes, making automation of the testing process essential.

2.5.3 Finding magnetic moment from measurement

The DC magnetic field emissions test is used to find the magnetic moment M from the magnetometer measurements performed during each step of the test. During the test, magnetic field B is measured for each of the six semi-axis in microTeslas. For each measurement distance, seen in Figure **5**, mean B-field values must be computed in microTeslas by following equations:

$$B_X = \frac{B_{(+X)} - B_{(-X)}}{2}, B_Y = \frac{B_{(+Y)} - B_{(-Y)}}{2}, B_Z = \frac{B_{(+Z)} - B_{(-Z)}}{2}$$

The measured B-field values must then be converted into magnetic moment M. For each measurement distance r, 3-axis magnetic moment components in Am^2 can be derived from the measured B-field using the following equations:

$$M_x = 5r^3 B_X, M_y = 5r^3 B_Y, M_z = 5r^3 B_Z.$$

Using calculated values M_x, M_y and M_z at distances r_1 and r_2 magnetic moment values M_1 and M_2 can be calculated:

$$M_1 = \sqrt{M_x(r_1)^2 + M_y(r_1)^2 + M_z(r_1)^2}$$

$$M_2 = \sqrt{M_x(r_2)^2 + M_y(r_2)^2 + M_z(r_2)^2}$$

The magnetic moment must be less than $0.001Am^2$, according to section 2.5.1. Based on the instrument's general dimensions, the closest measurement distance r for placing the magnetometers is around 10 cm. The B-field requirement can be calculated by:

$$B = \frac{M}{5r^3} = \frac{0.001}{5 \cdot (0.1)^3} = 0.2\mu T$$

3. Existing Helmholtz Coils

The Helmholtz coils hardware has been developed multiple times in the Tartu Observatory with the first iteration created by Hannes Haljaste in 2014 to test ESTCube-1 satellite on Earth before launch as well as to investigate satellite rotation algorithms[23]. It had one coil pair with a custom electronics board and control logic. Later on, during a 2015 student summer camp called Teadusmalev, students managed to build a Helmholtz coil cage with three pairs of coils, seen on Figure **6**. In the next 9 years, not a lot changed with the existing Helmholtz coils. Students had only made mechanical hardware for the 3-axis Helmholtz coils, but there had not been electronics or software development. Some students tried to make electronics board to control the coils, but they did not produce a working solution.

To replicate the rotational dynamics of orbiting satellites, the Helmholtz coils are required to produce a magnetic field with twice the intensity of Earth's magnetic field. The three pairs of Helmholtz coils exhibited slight variations in resistance. The X-axis coils had resistances of 22.73 and 22.86 Ω, the Y-axis measured 21.55 and 21.83 Ω and the Z-axis measured 20.44 and 20.48 Ω with radii 0.61 m, 0.58 m and 0.55 m, respectively. Each coil consisted of 135 turns. The supporting frame for the Helmholtz coils was constructed using 45 x 45 mm wooden poles that were attached to 9 mm plywood sheets from the top and bottom.[24]

Figure 6. Existing 3-axis Helmholtz coils

4. Aim and Objectives of the Thesis

Three axis Helmholtz coils have been in Tartu Observatory for more than a decade, but they have not been used or thoroughly tested and the documentation about them is deficient. For testing OPIC's qualification and flight models, utilizing the available Helmholtz coils presents a great opportunity to develop the experimental setup. Using the existing Helmholtz coils for DC magnetic field emission test would be very convenient, but the coils should be tested first to see if they would meet the requirements.

The goal of this Bachelor's thesis is to study the feasibility of performing the DC magnetic field emission test that is required for the OPIC instrument in-house at Tartu Observatory. The focus is on the magnetic field compensation and permanent field part of the DC magnetic emission test (steps 1, 3, 4 in section 2.5.2), because deperming (steps 2, 5 in section 2.5.2) needs special hardware development that can be created after analyzing the whole system and is thus out of the scope of the thesis. Objectives of the thesis are the following:

- Develop control logic for Helmholtz coils that can stabilize Earth's magnetic field.
- Develop additional hardware that would allow precise magnetometer placement.
- Evaluate the stability and uniformity of the magnetic field generated by the existing Helmholtz coils through magnetometer measurements.
- Analyze the Helmholtz coils' suitability for DC magnetic field emission test. If the existing Helmholtz coils turn out to be unsuitable, then define what would be required instead.

5. Hardware

When the thesis author started working with the Helmholtz coils, it was found that simple control can already be done by using a power supply. Since deperming was excluded from the scope of the thesis' practical work, then changing current direction was not required and using a standard laboratory power supply was sufficient. In order to create a stable magnetic field, like neutralizing Earth's magnetic field, Helmholtz coils need to produce a magnetic field in only one direction. This is still quite challenging, since it is necessary to control six coils simultaneously with high currents. But finding a power supply with 6 channels or using multiple power supplys to control Helmholtz seemed unnecessary. Three channel power supply NGE100 by Rohde & Schwarz NGE100 was chosen since all of its channels can go up to 32 volts and 3 amperes with a precision of 0.001 amperes.

The coil pairs could also be connected in series or in parallel to the channels. Connecting in series could ensure that they get the same current. But for calibrating the Earth's magnetic field parallel connections give more precision. With series connection the precision is same as power supply current precision of 0.001 A (1 mA). But for parallel connections the current is divided between two coils so the precision is 0.0005 A (0.5mA). Since coils resistance varies less than 2% or 0.3 ohms, then their current values for Earth's magnetic field compensation vary less than 1 mA which is negligible. When connecting the coils in parallel it should be checked that the current goes through them in the same direction. The coils should be connected to the power supply so that applying current will move the magnetic field strength towards zero. In case the magnetic field goes further from zero when applying current, coils are connected in the wrong direction and their polarity should be switched.

The connections between computer, magnetometers and power supply are shown in Figure **7**. These show the main control loop that was chosen for reading magnetic field data and controlling Helmholtz coils by power supply via USB serial connection.

5.1 Helmholtz underboard and magnetometer holder design

Previously, demo measurements were done by just placing a cardboard box in the middle of the Helmholtz coils and a magnetometer on top of the box, shown in Figure **8**. Neither the box nor the magnetometer was fixed to a certain place or angle in any way. That meant there was no way to know how far the sensor was from the center of the coils. Already, a small difference between sensors and coils' angles would mean that X- and Y-axis measurements give false

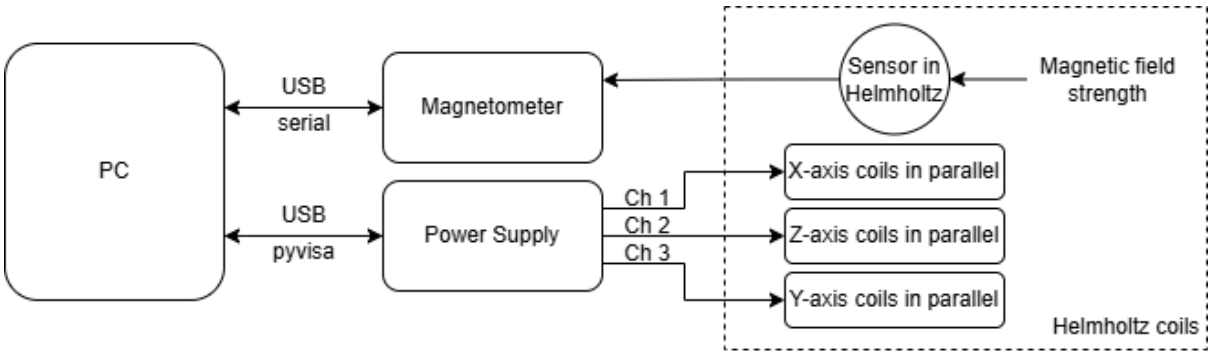

Figure 7. Hardware connection block diagram for magnetic field calibration

control inputs to the power supply. Because of this, it was decided to develop a mechanical solution on which 3D printed magnetometer holders could be attached to certain positions. The board had to be fixed to the Helmholtz coils' wooden frame, and holes had to be drilled to connect the magnetometer holder. This way magnetometer could be attached exactly to the center point of the Helmholtz coils to maximally stabilize the Earth's magnetic field, as seen in Figure **10**. Both the underboard and the magnetometer holder were designed using SolidWorks, a Computer-Aided Design (CAD) software with which the author had prior experience.

Figure 8. Helmholtz coils with magnetometer on a cardboard box

Figure 9. Helmholtz coils with twisted polyamide cord for finding the center

Figure 10. Helmholtz coils with underplate and magnetometer in the center

The underboard was designed after taking measurements from the Helmholtz coils' wooden frame. The board was milled out of birch plywood as wood does not affect the measurement

results. Wooden dowels were added to the edges to hold the plate in place. The CAD drawing of the board can be found in appendix Figure **26**.

The magnetometer sensor holder was designed through multiple iterations of prototyping. To get the design that would stay firmly around the magnetometer, different tolerances were iteratively tested with inner side lengths ranging between 25.15 x 32.4 and 25.4 x 32.8 mm. The images of prototypes can be found in appendix Figure **27**. The design with the smallest inner sides was chosen because it held the magnetometer tightly.

Once the underboard was ready to use, the focus shifted to prototyping the bottom part of the magnetometer holder that connects to the board. This part consists of 5 cylinder-shaped legs that aligned with the holes in the underboard. Having so many legs made sure that magnetometer would stay still and not move on the board. Different prototypes had legs with diameters ranging between 6.2 and 6.4 mm and can be found in appendix Figure **28**. The middle size, with 6.3 mm leg diameter was chosen because the connection was stable, but also allowed moving the magnetometer to a different place with ease. Magnetometer holder connection to the board can be found in appendix Figure **30**.

After the top and bottom connections were finished, they were connected to each other by a 197.5 mm long cylinder that allow placing the magnetometer as close to the magnetic field center as possible. The design of the magnetometer holder can be found in appendix Figure **29**. All the magnetometer holder prototypes were made with PLA filament using Bambu Lab P1S 3D printer.

The picture of the final setup can be seen in Figure **11**.

Figure 11. Magnetometers connected in test configuration to the underboard using magnetometer holders

6. Software

The first objective of the thesis was to develop control software that can neutralize the Earth's magnetic field. The requirement for the control logic software was to measure the magnetic field at the center of the Helmholtz coils with a magnetometer and use the measurements as a feedback for the power supply control. The first step in the software development was implementing remote control functionality for the magnetometer and power supply.

6.1 Magnetometer Control

For the magnetometer, a command for reading data was needed. Through reading Alphalab Inc. Data Acquisition Communication Protocol, the `stream_data` command was found, that can be used for getting the most recent data from the magnetometer[25]. In the stream data command in Figure **12**, the computer sends one command byte with a value of 0x03 and five bytes of dummy data to the magnetometer, after which the magnetometer replies with 6 bytes of data for all four datapoints (X-axis, Y-axis, Z-axis magnetic field measurements and the vectorized total magnetic field strength) and acknowledge byte 0x08.

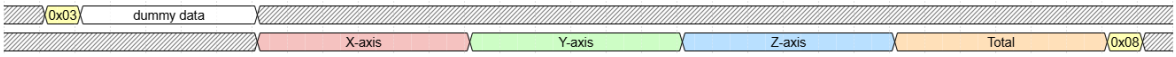

Figure 12. Stream_data command in bytes. The first line is the packet the PC sends to magnetometer and the second line is magnetometer's reply

Each datapoint had to be processed to obtain it in readable units (milligausses). As seen on Figure **13**, each datapoint is 48 bits long, first 12 bits are for configuration, then 4 bits for sign and decimal information and last 32 bits are the actual measurement value in milligauss. The configuration bits marked with I, F, H1, H2 and C, are not important in our context and will not be further explained. If the 13th bit was 1, then it meant that the sign was negative and data had to be multiplied with -1. The decimal place bits 14-16 could be converted into integers between 0-7, that showed how much data had to be shifted to the left or divided by a corresponding power of 10. After implementing the decimal place shift and sign bit logic, the result was magnetic field strength in milligausses.

Most of the time, when sending the stream data command, the magnetometer responded quickly, but there were times when the program got stuck, expecting to read magnetometer data, but not receiving any. For these occasions, a 1-second timeout for serial was added, so when receiving a data packet with a length of zero, then a new stream data command could be sent.

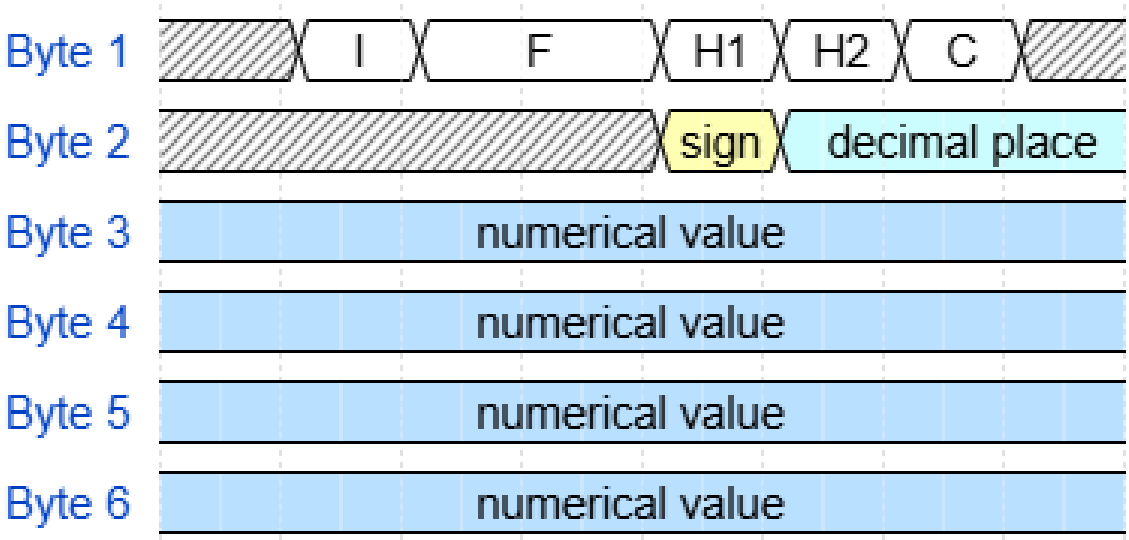

Figure 13. Datapoint composition in bits

6.2 Power Supply Control

For the power supply, there was need to give separate current inputs to all channels. The NGE100 user manual described multiple remote control options such as USB, LAN, WLAN, LXI, SCPI and VISA[26]. Since the thesis author had previous experience with VISA and it can be easily setup over USB connection, VISA interface was chosen.

Virtual instrument software architecture (VISA) is a widely used standardized software interface that is used for communicating with instruments from a computer. For Python there is PyVISA Python package, that allows controlling measurement devices using VISA interface.

After initializing the pyvisa resource manager and opening the correct USB port, power supply can be remotely controlled. Before changing the voltage and current, channel had to be selected and turned on. This can be done using INSTrument SELect ch_nr and OUTPut ON commands. After selecting channel, voltage and current values can be changed by VOLTage x and CURRent x commands. The power supply can control voltage with 0.01 volt precision and current with 0.001 Amper precision. If the voltage value is restricting current so that current is unable to reach the selected value, then the power supply is controlled by voltage. If current is restricting voltage, then power supply is controlled by current. Since Helmholtz coils should be controlled by current, then voltage was set to 32 V, the maximum value of the power supply, that will not be reached during calibration and subsequent control was performed with changing current.

6.3 Earth's magnetic field compensation in one axis

The implementation of the control logic for compensating the Earth's magnetic field was started by developing it for only one axis at first. Logic for a simple proportional controller can be found in Figure **14**. The controller takes one magnetometer measurement and if it differs from the zero field more than 0.1 milligauss then the new current value will be calculated. The magnetic field difference multiplied with a gain is added to the previous current value to find a new value where to set the power supply current. The value 0.001 was chosen as gain after testing the logic on the coils. Since the smallest step in current, 0.001 amperes changed the magnetic field a bit less than 1 milligauss, then 1 milligauss difference from the desired magnetic field should change the power supply current by smallest step of 0.001 amperes. If the power supply current value stays the same, then it is already at the best possible value and the coils are calibrated. After setting the new current value, new magnetometer measurement can be taken and the loop repeats itself. Coils will be calibrated when the magnetic field is less than 0.1 milligauss different from the neutralized field or current value stays the same.

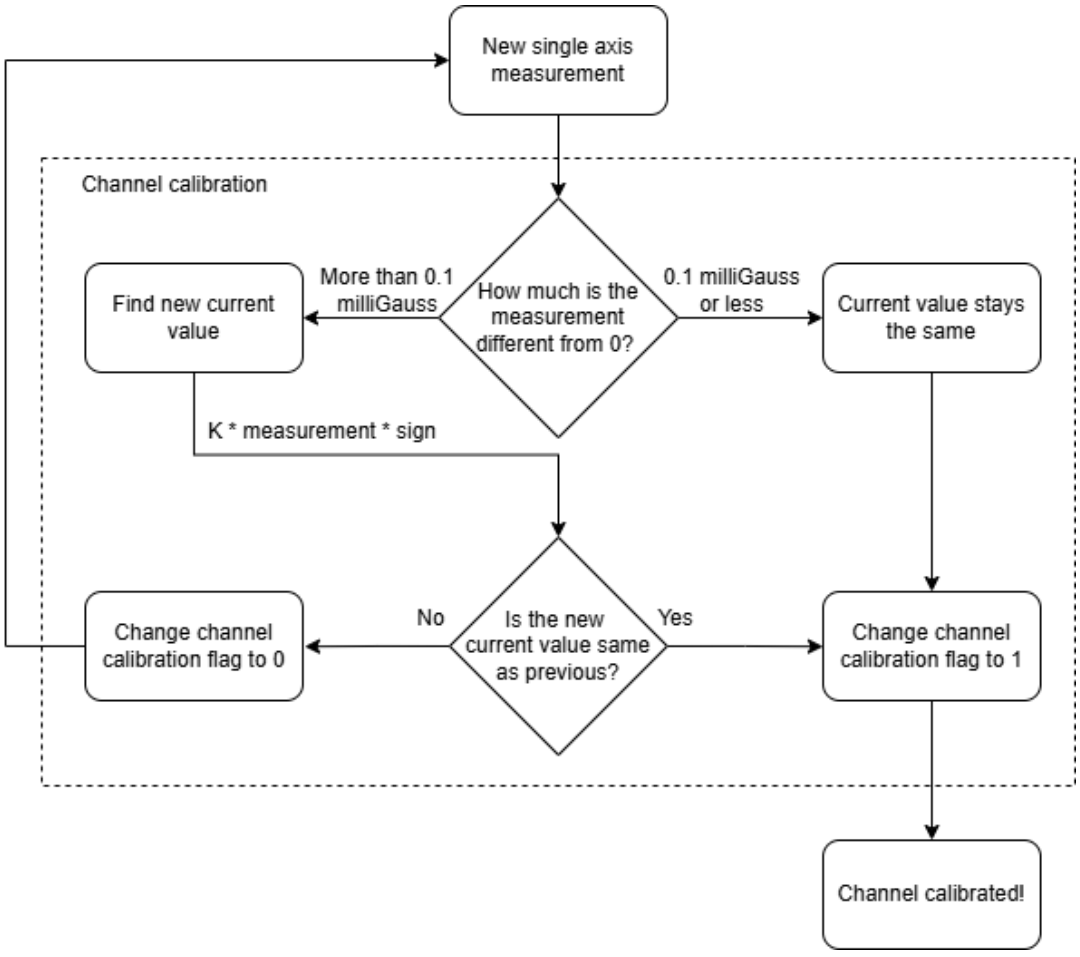

Figure 14. Earth's magnetic field neutralizing logic in one axis

6.4 Automated checks

Automated checks were implemented to map Helmholtz coils axes with channel numbers and check the direction of coil connections. Without them, magnetometer had to be always placed in the same direction, and there could be errors from reconnecting the power supply and Helmholtz coils with cables. A short function for checking axes connections was added before the calibration sequence, seen in Figure **15**.

This runs the same logic in a row for all channels. It takes one magnetic field measurement without power supply control, and then turns one power supply channel to 0.5 amperes to take a second magnetic field measurement. After that, it finds the absolute value between the first and the second measurement. Through finding the highest absolute value, it is visible which axis is influenced the most by a change in current and the dependency between channel number and axis can be saved into a variable. The two magnetometer measurements can also be used to determine the channel polarity. If the initial measurement is positive and the field strength decreases, or if it is negative and the field strength increases, the channels are correctly connected with a sign of +1 or -1, respectively. In case any channel is connected the wrong way user will get instructions on what connections to switch and the calibration sequence will not start.

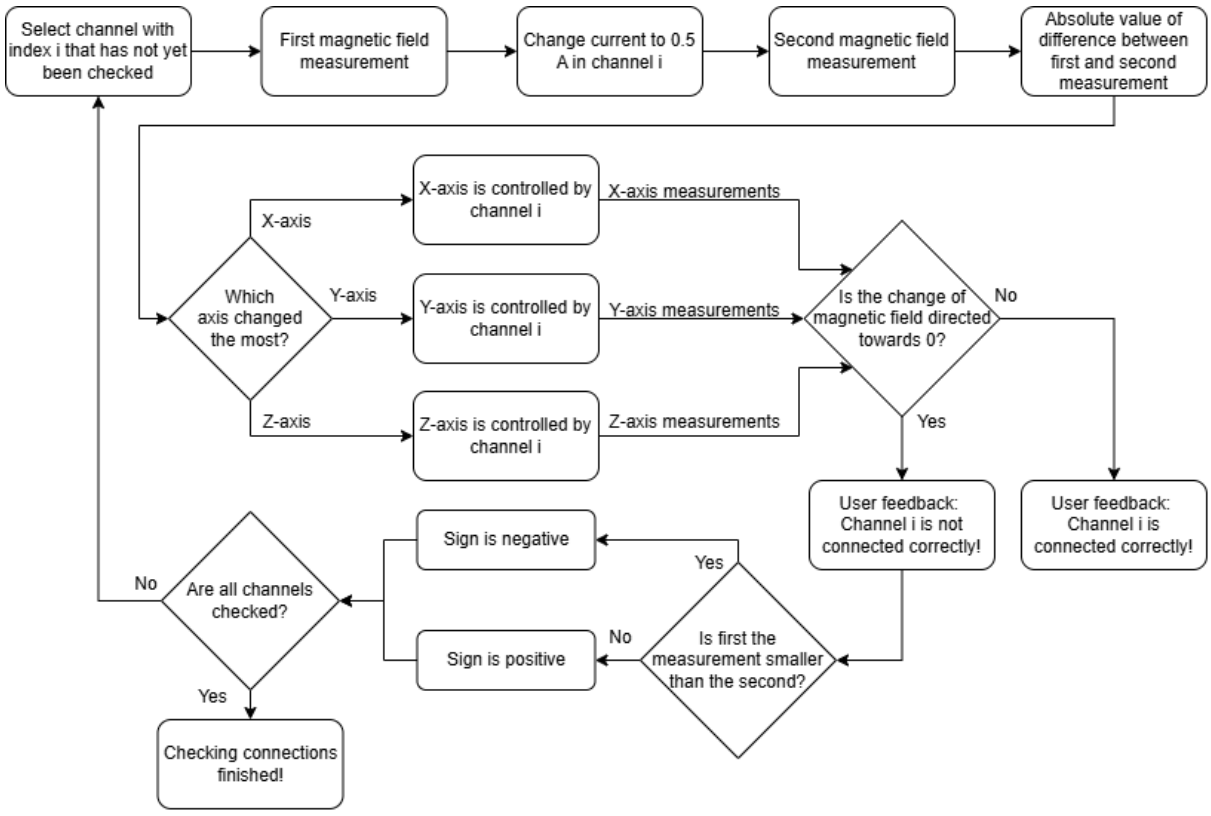

Figure 15. Automated checks logic

6.5 Earth's magnetic field compensation in three axis

After implementing the control logic in one axis, it was time to control all three axes simultaneously. The Earth's magnetic field compensation logic for three axes can be seen in Figure **16**. The logic runs the calibration algorithm on all axes separately, making it quite similar to one-axis control, although there are still some differences. The accuracy of the implemented controller was 1 milligauss, limited by the precision of the power supply's current output.

- First, the power supply channels had to be matched with the magnetometer axis they were controlling.
- Second, all the channels had to have an added sign bit to indicate whether the measured magnetic field should be added to or subtracted from the current value. If the magnetic field without Helmholtz control is positive, the magnetometer reading can be added directly, but if it is negative, the reading should be multiplied by -1 to prevent a negative current.
- Third, there needed to be logic for checking that the magnetic field is calibrated in all axes. In case of only some axis being calibrated, the calibration procedure had to be run again to compensate for the minor changes caused by other channels.
- Fourth, an additional changing channel command was needed after every iteration, since the current change command does not take the channel number as a variable.

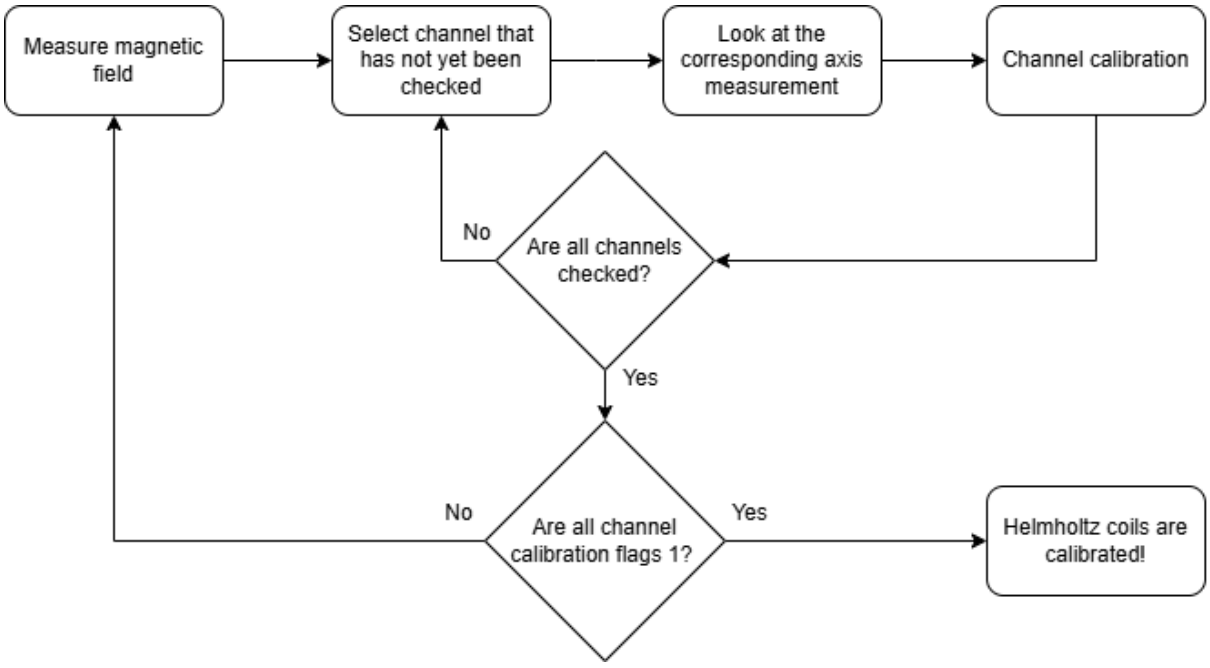

Figure 16. Earth's magnetic field neutralizing logic

7. Testing

The third objective of the thesis was to test the stability and uniformity of the created magnetic field using the existing Helmholtz coils. For the stability test it was decided to measure magnetic field in the center of Helmholtz coils for a long time. For the uniformity test, different positions in the middle of Helmholtz coils must be measured to map the magnetic field variation.

7.1 Stability test

The stability of the magnetic field generated by the Helmholtz coil was tested. For this, the magnetic field was calibrated to compensate the Earth's magnetic field, after which the field was measured every 10 seconds for an hour. The aim of the activity was to observe magnetic field fluctuations and give an estimate on how much the magnetic field changes due to temperature changes of the Helmholtz coils heating up. This information could be useful input in the future when the final test procedure for the DC magnetic emissions measurements is developed.

During the first measurement, the coils had already been subjected to prior testing, resulting in elevated temperatures. Consequently, the coil resistance remained relatively stable throughout the measurement, and magnetic field strength drifted between 0.2 and 1.03 milligauss. The average magnetic field strength was 0.7 milligauss, and X-,Y- and Z-axes averages were 0.45, 0.43 and 0.22 milligauss. All measured values fall below the power supply control threshold of 1 milligauss, , indicating that adjusting the power supply current value would not yield an improved level of calibration. The results obtained from the measurements are illustrated in Figure **17**.

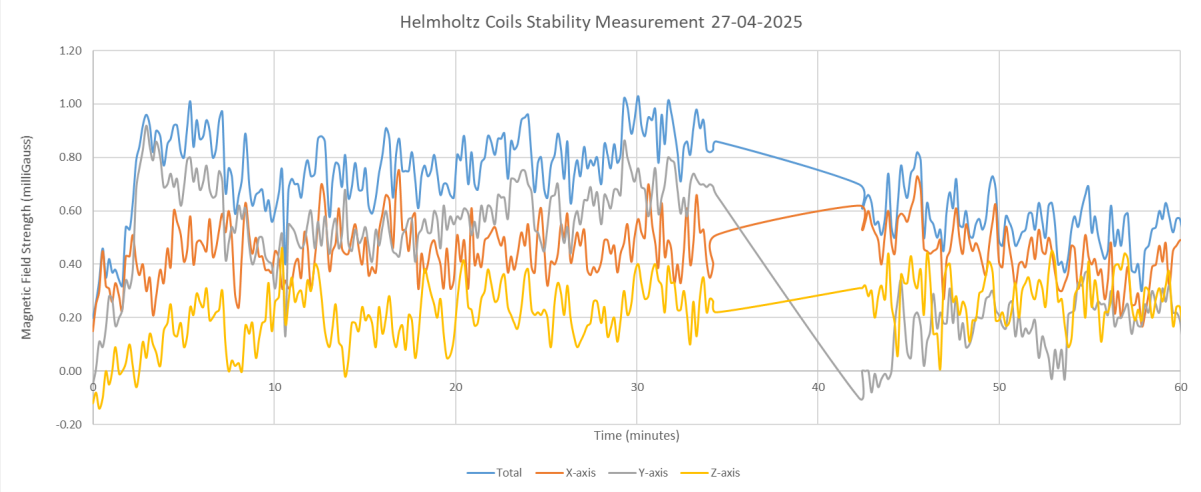

Figure 17. Stability measurement 1

The second measurement was conducted without prior use of the Helmholtz coils on the day of the measurement. As the coils had not yet heated up, their resistance increased during the measurement, resulting in a substantially larger variation in magnetic field strength values. Magnetic field strength ranged from 0.59 to 2.28 milligauss with an average of 1.66 milligauss. For compensation, X- and Y-axes get less than 0.1 amperes, so they do not heat up as much as the Z-axis, which gets around 0.35 amperes. In the first measurement, Z-axis magnetic field strength values ranged between -0.14 and 0.46 and multiple times during the measurement magnetic field reached exactly 0.00 milligauss. In the second measurement Z-axis magnetic field strength varied between 0.1 and 1.48 milligauss, with the average being 0.78. From this can be noted that it would be better to calibrate all axes again after approximately 10 minutes. But the second graph has weird jumps in magnetic field strength that happening at different times for the axis. The jumps seem to be around 0.8 milligauss up or down at the time and this could indicate changes in power supply current. Since the power supply can only give 0.001 amper precision and 0.001 difference changes the output around 1 milligauss, then already small fluctuations in power supply current can lead to visible differences in magnetic field measurements. Figure **18** displays the measurement data.

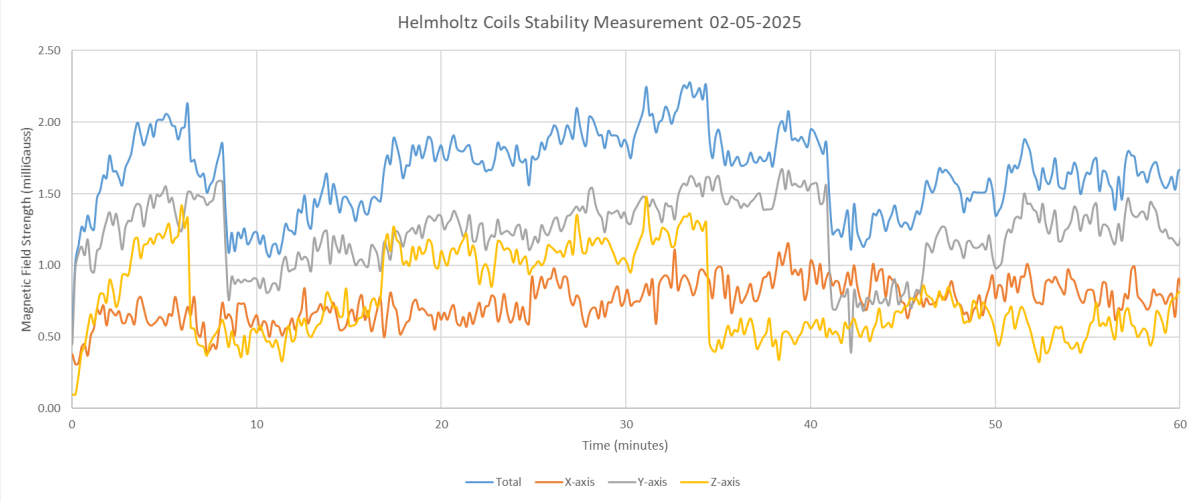

Figure 18. Stability measurement 2

Finally, a third stability measurement was performed. This time a periodic re-calibration of the magnetic field to compensate the Earth's magnetic field was implemented. As the coils' temperature increases during the operation, its resistance increases. This in turn affects the current in the coils which in turn affects the strength of the magnetic field. Re-calibration to the Earth's magnetic field was implemented to be performed every 15 minutes. The magnetic field strength stayed between 0.02 and 1.66 milligauss. The average magnetic field strength was 0.91

milligauss, and the X-, Y-, and Z-axes averages were 0.19, 0.32, and 0.30 milligauss. In the third measurement, Z-axis magnetic field strength values ranged between -0.48 and 1.41. This is more precise than the first measurement, and the values are according to the requirements below 2 milligauss, as described in section 2.5.3. The measurement results are shown in Figure **19**.

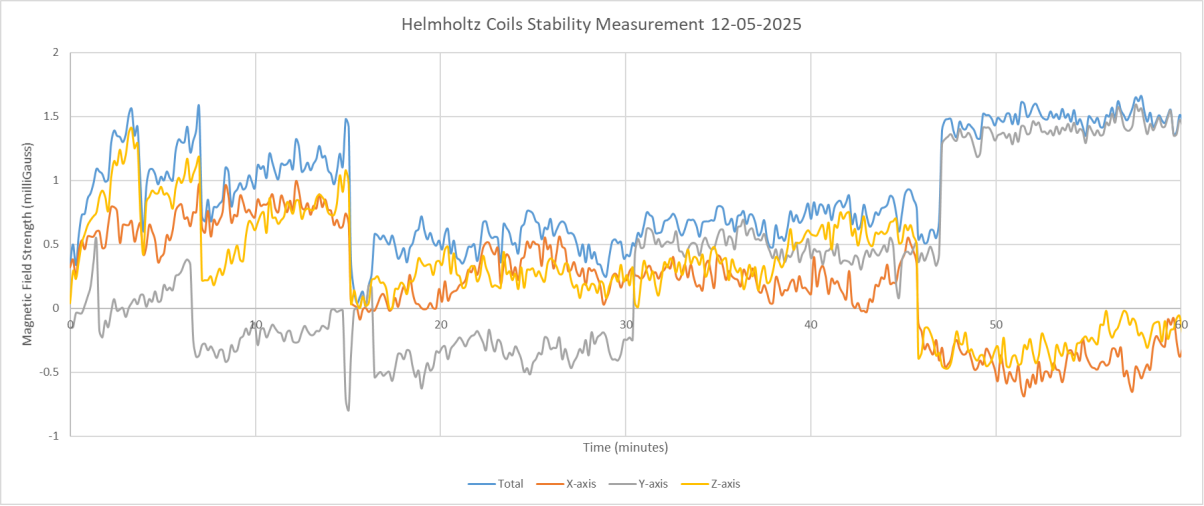

Figure 19. Stability measurement 3

7.2 Uniformity test

To determine the magnetic field uniformity, it was decided to measure the magnetic field at certain positions on a plane perpendicular to the Z-axis. The plane is located at an equal distance from both Z-axis coils. This meant that measurements could be done by placing the magnetometers in different places on the underboard. On the board, 21 x 15 positions were measured, which were on a grid after every 3 cm. For taking the measurements, the magnetometer was moved around the board by hand, and its position was given to the test program before every measurement. Both magnetic field data and position were saved to a CSV file. To account for the imperfect compensation of Earth's magnetic field, a measurement was taken at the desired position and compared with a reference measurement from the center point.

A 2D pixel plot illustrating the total magnetic field—derived from the combined X-, Y-, and Z-axis vectors—is shown in Figure **20**. The figure shows that the magnetic field is relatively uniform at the center of the Helmholtz coils in all axes, but at the edges, the field varies by more than 50 milligauss. In the Z-axis, the magnetic field is even more uniform. The magnetic field is even more uniform when considering only the Z-axis. Figure **21**, illustrates that the magnetic field difference remains under 10 milligauss within a circle of roughly 45cm in diameter. Since

the measurements are performed in the center of the Z-axis plane, it is expected to see quite a uniform area in the middle.

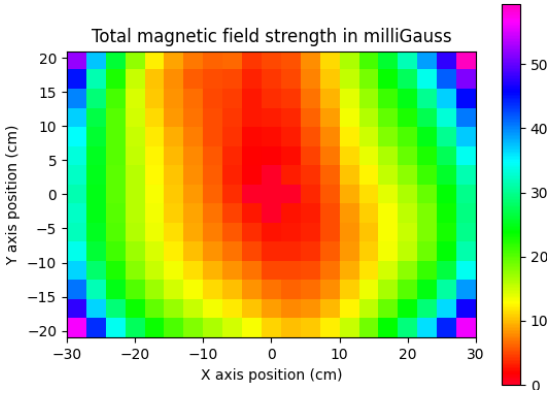

Figure 20. Total magnetic field over Helmholtz coil area

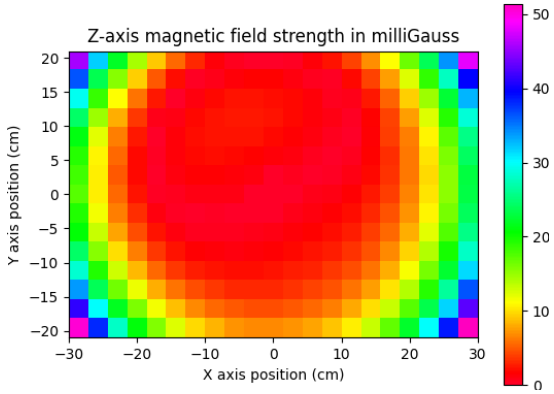

Figure 21. Z-axis magnetic field over Helmholtz coil area

The findings are not as interpretable when looking at the magnetic field in X- and Y-axes. The magnetic field should be the most uniform in the center of the area between corresponding coils. That would mean that in the Figure **22**, the coils are located in the top and bottom of the graph and there should be a visible horizontal line in the middle of the graph. For the Y-axis, the coils are located from left and right of the area being measured and there is a quite visible vertical line in the middle of the Figure **23**. Upon reviewing the graphs, Anomalies were observed in the X-axis data. After investigating the X-axis coils, it was visible that the coils are at a small angle from each other. The coils should be firmly attached to the wooden frame, but Figure **24** shows that one of the X-axis coils was 2.5 centimeters away from the frame.

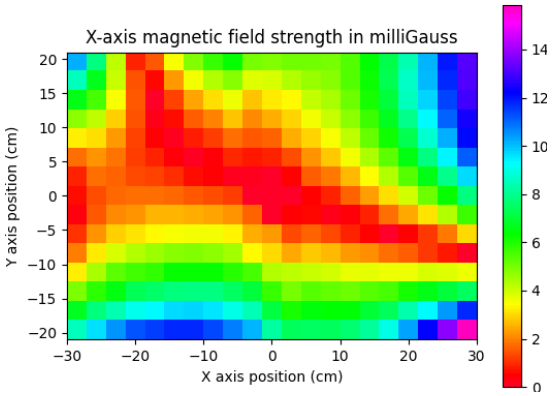

Figure 22. X-axis magnetic field over Helmholtz coil area

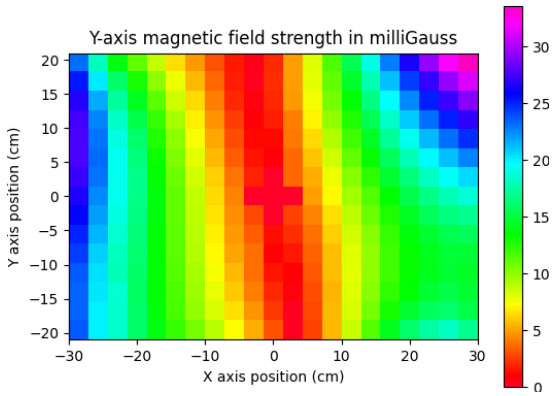

Figure 23. Y-axis magnetic field over Helmholtz coil area

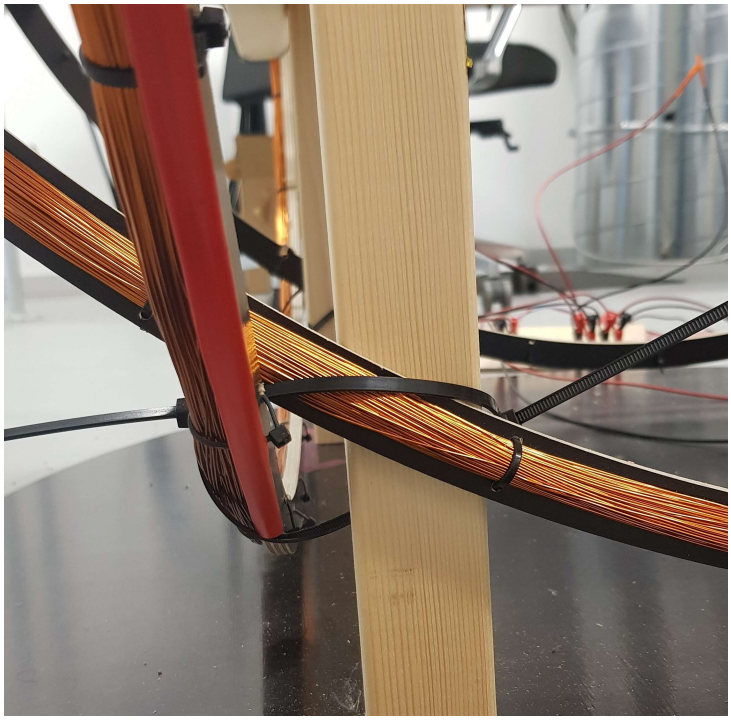

Figure 24. X-axis coil is visibly away from wooden frame

7.3 Magnetic field differences from calculations

The accuracy of estimating magnetic field measurements using theoretical equations was also evaluated. This involved measuring the change in magnetic field at the center of the Helmholtz coils for each axis when applying 0.1, 0.5, and 1.0 ampere currents. The calculations were performed using the formula for determining the magnetic field at the center of the coils, provided in section 2.4. As can be seen in Figure **25**, the computed and measured magnetic fields differ on average only about 1%.

Current	0.1 A			0.5 A			1.0 A		
	X-axis	Y-axis	Z-axis	X-axis	Y-axis	Z-axis	X-axis	Y-axis	Z-axis
Calculation (μT)	9.95	10.465	11.035	49.75	52.323	55.177	99.499	104.646	110.353
Measurement (μT)	9.589	10.462	10.95	49.337	52.911	55.779	99.059	105.813	111.809
Difference in %	-3.76473	-0.02868	-0.77626	-0.8371	1.1113	1.079259	-0.44418	1.102889	1.302221

Figure 25. Magnetic field strength calculations and measurements comparison

8. Recommendations towards a new Helmholtz setup

The fourth objective of the thesis to analyze the Helmholtz coils suitability for the test. This included defining requirements for a better system, in case the current solution is not deemed enough.

The work on the Helmholtz coils revealed that the current setup is not capable of creating a magnetic field with 300 microTeslas (3000 milligauss) required for the perming part of the DC magnetic field test described in section 2.5.2. The power supply channels are limited to 33 watts, which means according to the Power Formula $P = UI$ [27], the product of current and voltage cannot be more than 33. On average, the resistance of one coil is around 21.5 ohms and two coils in parallel are thus 10.75 ohms $\frac{1}{R} = \frac{1}{R_1} + \frac{1}{R_2}$. When combining this with the Ohms Law[28]: $I = \frac{U}{R}$, it is derived that $I = \sqrt{\frac{33}{10.75}}$. This current is then divided by two coils leaving both coils with around 0.875 amperes at around 18.8 volts. Physical tests showed that the magnetic field change with such currents was below 200 microTesla (2000 milligauss). Using 0.58 m as average coil radius and 135 as number of turns as introduced in section 3, the magnetic field at the center of the Helmholtz coils can be calculated by equation from section 2.4:

$$B(0) = (\frac{4}{5})^{3/2} \cdot \frac{4\pi \cdot 10^{-7} \cdot 135 \cdot 0.875}{0.58} \approx 183.130\mu T$$

When generating larger magnetic fields, the coils should be connected in series rather than in parallel. In this case, the power supply's voltage would become the bottleneck. Connecting the coils in series leads to a total resistance equal to the sum of the individual resistances ($R = R_1 + R_2$), which is approximately 43 ohms. According to Ohm's Law, the resulting current is approximately 0.744 amperes, which is even lower than when the coils are connected in series. Standard power supplies typically do not exceed 32 volts, so a specialized power supply is required. To evaluate its feasibility, two power supplies were connected in series to enable a higher voltage range. With this configuration, it was possible to reach 52.73 volts and 1.224 amperes. A higher voltage range makes it more likely to reach 300 microteslas:

$$B(0) = (\frac{4}{5})^{3/2} \cdot \frac{4\pi \cdot 10^{-7} \cdot 135 \cdot 1.224}{0.58} \approx 256.172\mu T$$

Other than the power supply, the coils themselves should also be changed. Since the coils were originally designed to generate magnetic field strengths comparable to that of Earth's [24], their resistance limits their capability to produce stronger magnetic fields. Using coils with lower resistance could enable the generation of higher magnetic field strengths. If the resistance of the

coils were 2 x lower (around 10.75 ohms), then the voltages could also be 2 x lower to get the same current. To get a field with 300 microTeslas, the coils should be controlled with at least 1.5 amperes.

$$B(0) = (\frac{4}{5})^{3/2} \cdot \frac{4\pi \cdot 10^{-7} \cdot 135 \cdot 1.5}{0.58} \approx 313.937\mu T$$

To use the existing power supply with 1.5 amperes below 33 watts, the voltage should be 22 volts or less: $U = P/I$ According to the Ohms Law, coils resistance should be 14.(6) ohms in series, so one coil should be below 7.(3) ohms. For reaching the magnetic field strength required in the deperming part described in section 2.5.2, the current should be even more than 10 times higher.

Having coils with lower radii would also help create a stronger magnetic field. If the coils had half the current radius (around 0.29 m), then the magnetic field between them would be 2 times higher, and OPIC could still fit between the Helmholtz coils with magnetometers. A smaller coil radius typically results in reduced magnetic field uniformity. However, when using industrially manufactured Helmholtz coils, the uniformity is generally specified by the manufacturer, allowing for verification of coils suitability for the intended application. A smaller coil radius would not solve the problem regarding the power supply capabilities, but would raise the magnetic field strength in the desired direction.

When the coils are already changed, the entire structure of existing Helmholtz coils could be changed. The frame is not stable and even with the added underboard could be shaken quite easily. As seen during the uniformity test not all coils are attached properly, which causes disturbances in the magnetic field.

Constructing a new structure and coils would be cumbersome, so the author of the thesis recommends purchasing a 3-axis Helmholtz coil system from reputable suppliers such as DexinMag[29], The EMC Shop[30], Schwarzbeck[31], or other manufacturers of industrial-grade Helmholtz coils. Assuming Helmholtz coils with a 30 cm radius, 100 turns, and a resistance of 1 ohm per coil, a 32-volt power supply would produce a current of 16 amperes, generating a magnetic field that meets the required strength:

$$B(0) = (\frac{4}{5})^{3/2} \cdot \frac{4\pi \cdot 10^{-7} \cdot 100 \cdot \frac{32}{2}}{0.3} \approx 4795.607\mu T$$

Furthermore, since regular power supply do not typically provide 16 amperes of current, the author of the thesis recommends using a power supply with a higher current capacity. Higher current is preferred to higher voltage, because only the current affects the magnetic field.

However, a DC supply would suffice, as the necessary Alternating Current (AC) can be generated using custom electronics.

After finding suitable Helmholtz coils and a power supply that would allow control in the desired area, custom electronics should be developed. The electronics should incorporate an analog control block, utilizing multiple operational amplifiers for each coil, to enable precise control of the magnetic field. It has to support generating an oscillating magnetic field with a frequency of 2.5 Hz to 5 Hz. This would be required for the deperming process. When selecting components, emphasis should be placed on maintaining the precision of the Helmholtz control to ensure compliance with the high accuracy required for magnetic field measurements. Aditionally, since the device must be capable of handling AC, a protective solution for safeguarding the electronics against reverse current should be implemented.

A custom PCB could be designed to deliver a precise and stable current, so that changes in coils resistance would not affect the current supplied to the coils. As a result, feedback from the magnetometers would not be necessary, since the system would maintain the required current, which can be calculated in advance to achieve the desired magnetic field strength along each axis. This approach is particularly important for implementing the deperming process, where currents must be accurately mapped to corresponding magnetic field strengths to enable the creation of a custom profile. Once established, this profile could be executed during testing without the need for real-time feedback from the magnetometers.

9. Conclusion

The goal of this thesis was to study the feasibility of performing the DC magnetic field emissions test for OPIC in-house in Tartu Observatory. The main focus was on the Earth's magnetic field compensation part of the DC magnetic field emissions test. The thesis analyzed the suitability of existing Helmholtz coils, which had already been developed by students, but had not been properly documented or tested. All of the listed objectives were met:

- A control logic for stabilizing the Earth's magnetic field with Helmholtz coils was developed.
- Additional hardware that would allow precise magnetometer placement was developed and manufactured. There is now a wooden underboard and 3D printed holders for the magnetometer's sensors.
- The stability and uniformity of the created magnetic field using the existing Helmholtz coils was tested and analyzed. Furthermore, it was verified how accurately the generated magnetic field can be calculated.
- The suitability of the existing Helmholtz coils for DC magnetic field emission test was analyzed. Possible improvements were defined.

For performing the DC magnetic field emissions test, the current setup is not sufficient. It is not possible to reach the magnetic field strength needed. The power supply should have a wider voltage and current range. The Helmholtz coils should have lower resistance and could be smaller in size. A custom-designed electronics board should be developed to enable precise control of the oscillating magnetic field.

Acknowledgements

I would like to express my sincere gratitude to Sten Salumets, my thesis supervisor, for providing invaluable guidance and expertise throughout this project.

Additionally, I would like to thank the mentors from Tartu Observatory and Tudengisatelliit for their insightful discussions and constructive feedback.

Special thanks to my fellow students for their encouragement and for enduring this journey alongside me.

Finally, I would like to thank my family and friends for their continuous support.

References

[1] Common European Research Classification Scheme (CERCS) Teadusvaldkondade ja -erialade klassifikaator. https://wiki.ut.ee/download/attachments/16581162/Common%20European%20Research%20Classification%20Scheme.pdf.

[2] ESA Requirements and standards. ESA. https://www.esa.int/Enabling_Support/Space_Engineering_Technology/Requirements_and_standards.

[3] Sauser B. J., Reilly R. R., and Shenhar A. J. Why projects fail? How contingency theory can provide new insights–A comparative analysis of NASA's Mars Climate Orbiter loss. *International Journal of Project Management* 27.7 (2009), pp. 665–679.

[4] Desai P. N. and Lyons D. T. Entry, descent, and landing operations analysis for the genesis entry capsule. *Journal of Spacecraft and Rockets* 45.1 (2008), pp. 27–32.

[5] Blackburn M., Busser R., Nauman A., Knickerbocker R., and Kasuda R. Mars Polar Lander fault identification using model-based testing. *Proceedings 26th Annual NASA Goddard Software Engineering Workshop*. 2001, pp. 128–135. DOI: 10.1109/SEW.2001.992666.

[6] Reinhard R. The Giotto encounter with comet Halley. *Nature* 321 (May 15, 1986), pp. 313–318. DOI: https://doi.org/10.1038/321313a0.

[7] Accomazzo A., Ferri P., Lodiot S., Pellon-Bailon J.-L., Hubault A., Porta R., Urbanek J., Kay R., Eiblmaier M., and Francisco T. Rosetta following a living comet. *Acta Astronautica* 126 (2016). Space Flight Safety, pp. 190–198. DOI: https://doi.org/10.1016/j.actaastro.2016.04.023. https://www.sciencedirect.com/science/article/pii/S009457651630090X.

[8] Snodgrass C. and Jones G. The European Space Agency's Comet Interceptor lies in wait. *Nature Communications* 10.5418 (Nov. 28, 2019). DOI: https://doi.org/10.1038/s41467-019-13470-1.

[9] Jones G., Snodgrass C., and Tubiana C. The Comet Interceptor Mission. *Space Science Reviews* 220.9 (Jan. 24, 2024). DOI: https://doi.org/10.1007/s11214-023-01035-0.

[10] Tinetti G., Drossart P., and Eccleston P. A chemical survey of exoplanets with ARIEL. *Experimental Astronomy* 46 (Sept. 11, 2018), pp. 135–209. DOI: https://doi.org/10.1007/s10686-018-9598-x.

[11] Pajusalu M., Kivastik J., Iakubivskyi I., and Slavinskis A. Developing autonomous image capturing systems for maximum science yield for high fly-by velocity small solar system body exploration. Oct. 2020.

[12] Space Camera Head CASPEX 4M. 3D plus. https://www.3d-plus.com/products/4mpx-space-camera-heads/.

[13] Stöhr J. and Siegmann H. C. Magnetism. *Solid-State Sciences. Springer, Berlin, Heidelberg* 5 (2006), p. 236.

[14] Grant I. S. and Phillips W. R. Electromagnetism. 2nd ed. The Manchester Physics. John Wiley & Sons, 2008.

[15] Lanza R. and Meloni A. The Earth's magnetic field. Springer, 2006.

[16] The Earth's Magnetic Field: An Overview. Geomagnetism BGS (British Geological Survey). http://www.geomag.bgs.ac.uk/education/earthmag.html#_Toc2075549.

[17] Coey J. Permanent magnet applications. *Journal of Magnetism and Magnetic Materials* 248.3 (2002), pp. 441–456. DOI: https://doi.org/10.1016/S0304-8853(02)00335-9.

[18] Evans R. H. "Magnetic Cleanliness". *2nd Symposium and Technical Exhibition on Electromagnetic Compatibility, Montreux*. 1977, pp. 183–188. DOI: 10.23919/EMC.1977.10797891.

[19] Bronaugh E. L. Helmholtz coils for calibration of probes and sensors: limits of magnetic field accuracy and uniformity. *Proceedings of International Symposium on Electromagnetic Compatibility*. Atlanta, GA, USA: IEEE, 1995, pp. 72–76. DOI: 10.1109/ISEMC.1995.523521.

[20] Helmholtz Coils. HyperPhysics, Electricity and Magnetism. http://hyperphysics.phy-astr.gsu.edu/hbase/magnetic/helmholtz.html.

[21] ECSS-E-ST-20-07C Electromagnetic compatibility standard. Version Rev.2. Jan. 3, 2022. https://ecss.nl/standard/ecss-e-st-20-07c-rev-2-electromagnetic-compatibility-3-january-2022/.

[22] 3-Axis Magnetoresistive Milligauss Meter MR3. AlphaLab Inc. https://www.alphalabinc.com/products/mr3/.

[23] Haljaste H. Magnetvälja simulaatori arendamine satelliidi ESTCube-1 testimiseks. Thesis archive. Tartu: University of Tartu, 2014. https://dspace.ut.ee/server/api/core/bitstreams/841692d2-2b0b-4058-acfb-903f1db9224b/content.

[24] Tudengisatelliit internal documentation, "Magnetic field emulation equipment". Oct. 11, 2022. https://confluence.tudengisatelliit.ut.ee:8433/spaces/EC2AOCS/pages/25428945/A.6.1.+Magnetic+field+emulation+equipment.

[25] Alphalab Inc. Data Acquisition Communication Protocol. https://www.alphalabinc.com/wp-content/uploads/2018/02/alphaapp_comm_protocol.pdf?srsltid=AfmBOordg-6KXaPj_crlt1TzAv7FotcJElRtvJQ25K8qsCB1tMq2tCe1.

[26] R&S®NGE100 Power Supply User Manual. 2017. https://www.batronix.com/files/Rohde-&-Schwarz/Power-Supplies/NGE/NGE100_User_Manual_en.pdf.

[27] Glisson T. H. Introduction to Circuit Analysis and Design. USA: Springer, 2011. 113-115.

[28] Millikan R. A. and Bishop E. S. Elements of Electricity. American Technical Society, 1917. 54 pp.

[29] Magnetic Field Source: Helmholtz Coils. Dexinmag. https://www.dexinmag.com/ProductInfoCategory?categoryId=215088&PageInfoId=0.

[30] Schloder MGA_HCST_50-28 50 / 46 / 42 cm Helmholtz Coil. The EMC Shop. https://theemcshop.com/emc-test-equipment/transient-generators/magnetic-field-generators/schloder-mga_hcst_50-28-50-46-42-cm-helmholtz-coil/.

[31] Helmholtz Coils. Schwarzbeck. https://www.schwarzbeck.de/en/helmholtz-coils-radiating-loops/helmholtz-coils.html.

Appendices

The following images depict the hardware developed for mounting magnetometers within the Helmholtz coil setup.

- Figure **26** displays the underboard that was designed to position magnetometers at precise locations inside the coils.
- Figure **27** shows various prototypes of the magnetometer sensor holder prototypes.
- Figure **28** contains a collection of magnetometer-to-board connections, each with different tolerance levels.
- Figure **29** features the final design of the magnetometer holder.
- Figure **30** shows how the magnetometer holders are attached to the underboard.

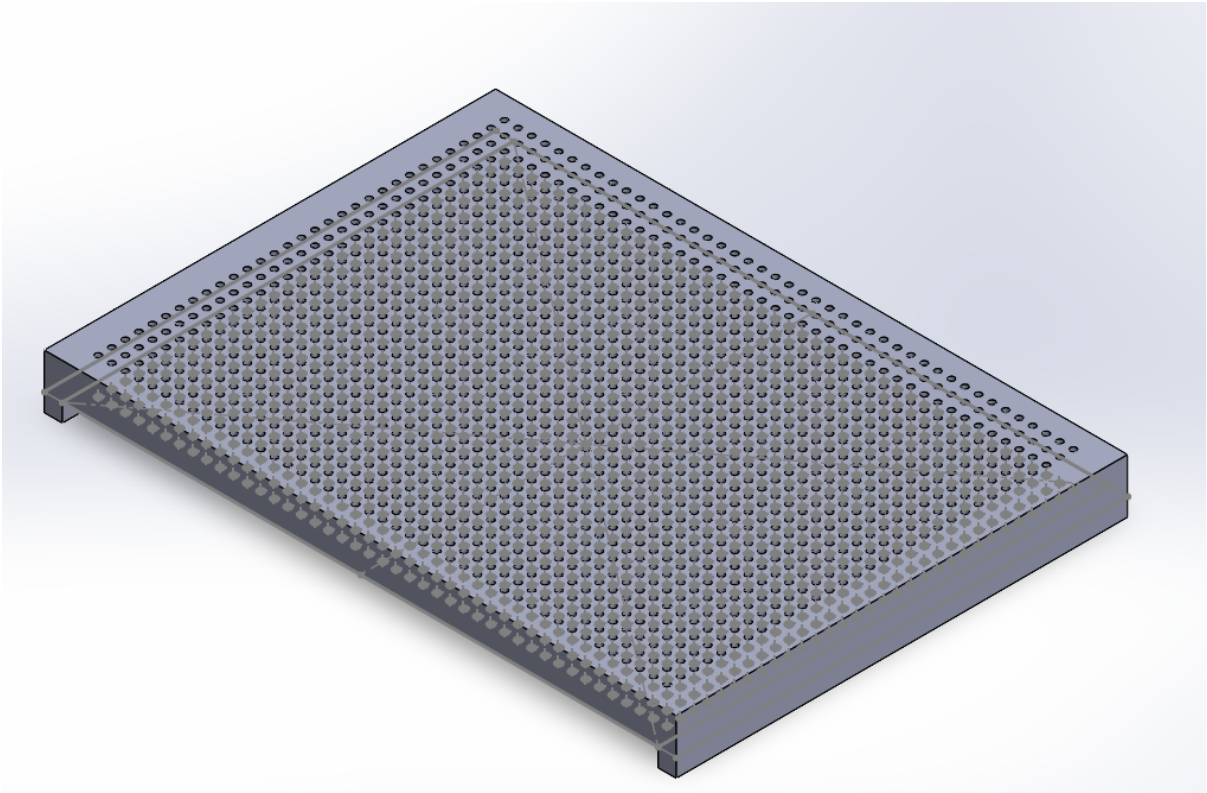

Figure 26. Drawing of Helmholtz underboard

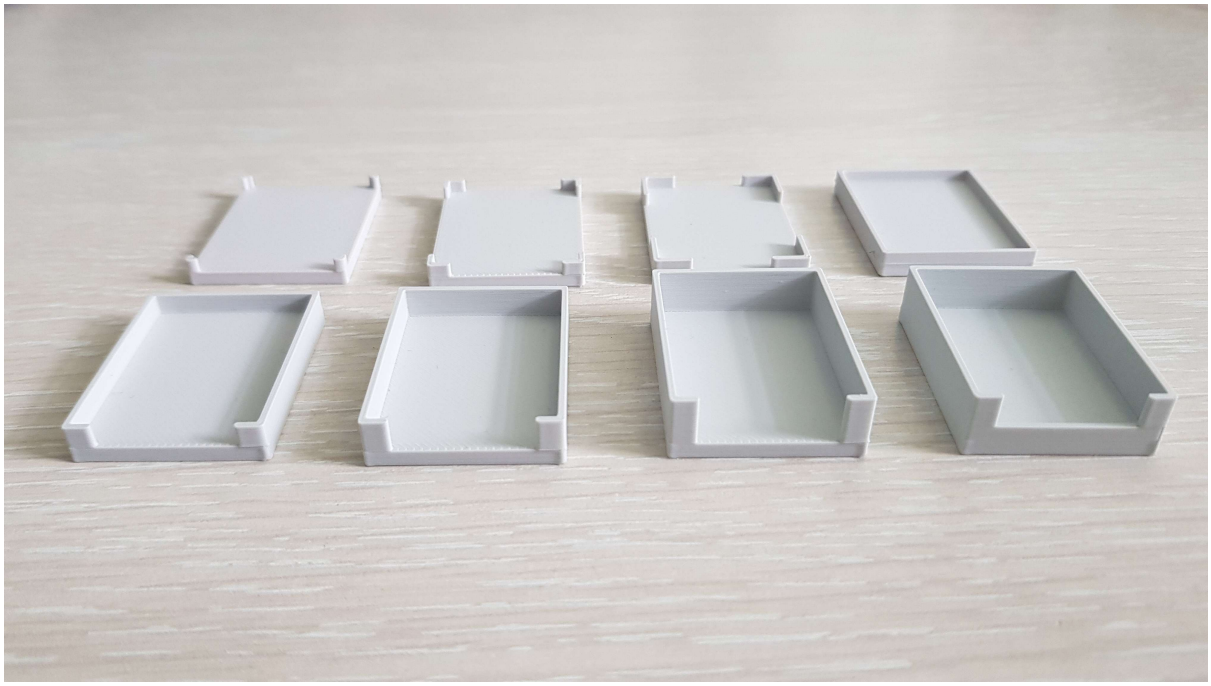

Figure 27. Prototypes of magnetometer holder connections to the magnetometer

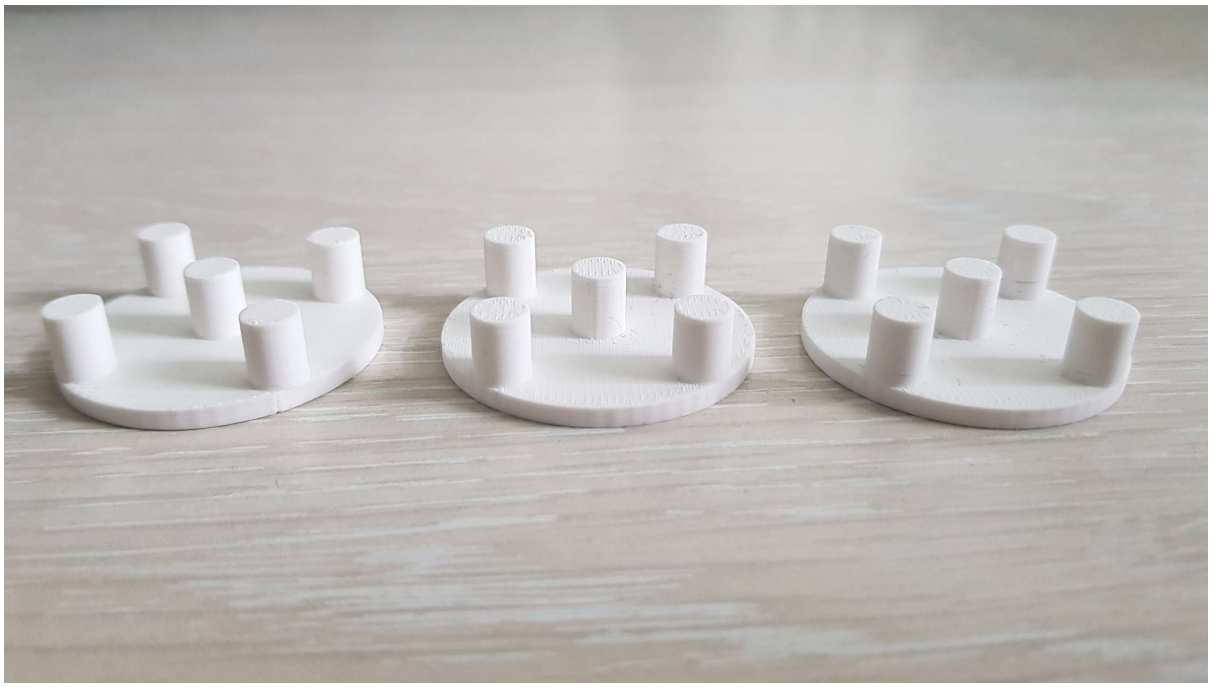

Figure 28. Prototypes of magnetometer holder connections to the board

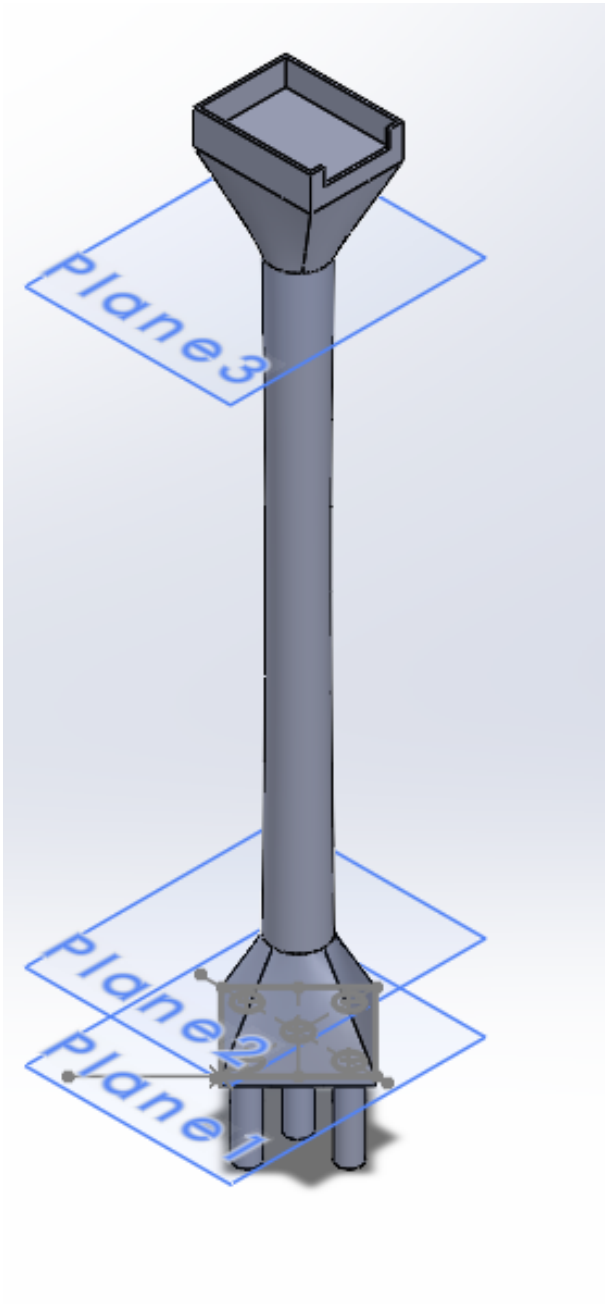

Figure 29. Magnetometer holder Drawing

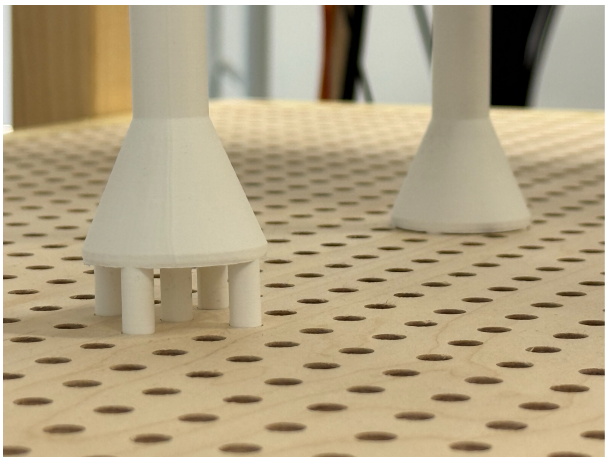

Figure 30. Magnetometer holders connecting to underboard

Non-exclusive licence to reproduce the thesis and make the thesis public

I, Michelle Lukken,

1. grant the University of Tartu a free permit (non-exclusive licence) to reproduce, for the purpose of preservation, including for adding to the digital archives of the University of Tartu until the expiry of the term of copyright, my thesis

   "Feasibility Study of Performing the DC Magnetic Field Emission Test for OPIC with Helmholtz Coils in Tartu Observatory",

   supervised by Sten Salumets;

2. grant the University of Tartu a permit to make the thesis specified in point 1 available to the public via the web environment of the University of Tartu, including via the digital archives, under the Creative Commons licence CC BY NC ND 4.0, which allows, by giving appropriate credit to the author, to reproduce, distribute the work and communicate it to the public, and prohibits the creation of derivative works and any commercial use of the work until the expiry of the term of copyright;

3. am aware of the fact that the author retains the rights specified in points 1 and 2;

4. confirm that granting the non-exclusive licence does not infringe other persons' intellectual property rights or rights arising from the personal data protection legislation.

Michelle Lukken

15/05/2025